

1 **Álvarez-Rodríguez, J., M.C. Llasat, T. Estrela 2019. Development of**
2 **a hybrid model to interpolate monthly precipitation maps**
3 **incorporating the orographic influence. Int J Climatol. 2019;1–14.**
4 **DOI: 10.1002/joc.6051**

5
6 **Development of a hybrid model to interpolate monthly**
7 **precipitation maps incorporating the orographic influence**

8
9 J. Álvarez-Rodríguez (a), M.C. Llasat (b, c), T. Estrela (d, e)

10
11 (a) Tagus River Basin Authority. Spanish Ministry of Energy, Environment and
12 Climate Change. Avda. De Portugal, 81. Madrid 28011. Spain

13 (b) Department of Applied Physics, Universitat de Barcelona, C/ Martí i Franqués,
14 1, 08028 Barcelona, Spain

15 (c) Water Research Institute (IDRA), University of Barcelona

16 (d) Júcar River Basin Authority, Ministry of Food and Fishing, Agriculture and
17 Environment, Av/ Blasco Ibañez 48, 46010 Valencia, Spain

18 (e) Instituto de Ingeniería del Agua y Medio Ambiente (IIAMA) de la Universitat
19 Politècnica de València, Spain.

20
21 *Corresponding author at:* Tagus River Basin Authority. Spanish Ministry for the
22 Ecological Transition. Avda. De Portugal, 81. Madrid 28011. Spain.

23 Tel.: +34 91 453 96 43; fax: +34 91 470 03 04

24 E-mail address: javier.alvarez@chtajo.es (J. Álvarez-Rodríguez)

Abstract

26

27

28

29

30

31

32

33

34

35

36

37

38

39

40

41

42

43

44

45

46

47

48

49

This paper proposes an interpolation model for monthly rainfall in large areas of complex orography. It has been implemented in the Iberian Peninsula (continental territories of Spain and Portugal), Balearic, and Canary Islands covering a territory of almost 600.000 km². To do this a dataset that comprises a total number of 11,822 monthly precipitation series has been created (11,042 provided by the Spanish Meteorological Agency and 780 provided by the National Water Resources Information System of the Portuguese Water Institute). The dataset covers the period from October 1940 until September 2005. The interpolation model has been based on the assumption of two different components on monthly precipitation. The first component reflects local and seasonal characteristics and 24 different mean monthly precipitation maps (12) and standard deviations maps (12) compose it. It considers the varying influence of physiographic variables such as altitude and orientation. The second precipitation component reflects the synoptic pattern that dominated each month of the series and it is composed by series of anomalies of monthly precipitation (780). Anomalies have been interpolated by means of ordinary kriging once local spatial continuity was assumed. Gridded maps of each variable have been developed at 200 m resolution following a hybrid methodology that implements two different interpolation techniques. The first technique applies a regression analysis to derive maps depending on altitude and orientation; the second one is a weighting technique to consider the non-linearity of the precipitation/altitude dependence. Cross validation has been applied to estimate the goodness of both techniques. Results show an average annual precipitation of 655 mm/year. Although this figure is only 4% less than the estimate of MAGRAMA (2004), regional and local

50 differences are highlighted when the spatial distribution is considered. The model
51 constitutes a comprehensive implementation considering the availability of historical
52 records and the need of avoiding slow calculations in large territories.

53 **1 Introduction and objectives**

54 The analysis and validation of interpolation procedures of precipitation is a topic
55 widely discussed in the fields of meteorology and hydrology (Daly et al., 2017; Singh
56 et al., 1995; World Climate Programme, 1985; Linsley et al., 1949). Basic data are
57 precipitation records of rain gauges, particularly when the studies are focused on
58 historical periods prior to the development of remote observation techniques (radar
59 and satellite). Due to the scarcity of records in areas where the variability of
60 precipitation is greater (Lloyd, 2005), precipitation estimation is carried out
61 considering the influence of physiographic factors and the spatial continuity of
62 precipitation, combining statistical and experimental methodologies (Hanson, 1982),
63 as well as physically based models (Barstad et al., 2007; Rotunno and Ferretti,
64 2001). Linear or multivariate regression models are used to construct statistical
65 relationships between precipitation and some physiographic variables such as
66 altitude, orientation, slope of the terrain, distance to water masses or altitude of
67 nearby mountainous areas. These factors are directly related to the triggering effect
68 and a forced uplift when wind direction and terrain's slope interact. Besides, the
69 influence of orography is also reflected in the shield effect and in the driving effect of
70 humid air masses through a complex topography (Bookhagen and Burbank, 2006;
71 Barros et al., 2004; Dhar and Nandargui, 2004; Marquínez et al., 2003; Hay et al.,
72 1998).

73 The methods of interpolation have been classified between deterministic or
74 stochastic, although the analysis of some reveals conceptual similarities. The
75 stochastic approach shows a formal definition to deal properly with uncertainties of
76 record measurement or those derived from the complexity of the physical processes
77 involved in precipitation generation mechanisms. However, variables such as
78 precipitation are not stationary and depend on a high number of local non-stationary
79 factors. The elementary predictive variable in the interpolation schemes is distance
80 to available records. Interpolation methods use it not only explicitly, but also through
81 the selection of records and the formulation of measures of spatial continuity.
82 Location allows the definition of altitude, orientation, slope, etc. to be used as
83 predictive variables.

84 In addition to the study of physiographic variables influencing precipitation,
85 interpolation models explicitly incorporate the evaluation of the spatial continuity by
86 means of covariances, polynomial structures, splines, variational approach,
87 quadratic function and adjustment criteria such as error and variance minimization
88 (Tobin et al. 2011; Naoum and Tsanis, 2004a and 2004b; Goovaerts, 2000;
89 Martínez-Cob, 1996; Weber and Englund, 1994 and 1992; Tabios III and Salas,
90 1985; Creutin and Obled, 1982; Gambolati and Volpi, 1979). Although there are a
91 large number of interpolation models, the question of the optimal or the best model
92 cannot be answered straightforwardly. Gómez-Hernández et. al. (2001) concluded
93 that complex models formally capable of integrating different types of relationships
94 and models of continuity in a rigorous manner such as kriging or the variational
95 approach (Mitas and Mitasova, 1988), do not guarantee obtaining better results than
96 those derived from simpler models. A typical example is the Thiessen methodology

97 (Thiessen, 1911), that filters out redundancies based exclusively on the
98 extrapolation of each record to the closest area (Falivene et al., 2010; Isaaks and
99 Srivastava, 1989). However, the goodness of an interpolation model depends largely
100 on the spatial variability of the precipitation event considered and on the density and
101 representativeness of the ground stations network. It is to say, it depends both on
102 the absence of records in places where the variability of precipitation is greater, as
103 occurs in the mountains and the coast, but also on the redundancy of data recorded
104 at close locations. Furthermore, it depends on the temporal step of the study,
105 considering that the complexity of the precipitation variability increases the shorter
106 the time interval is, and the random component becomes predominant. Particularly,
107 the lack of data in mountainous areas does not make it advisable to use techniques
108 whose parameterization is sensitive to the lack of information.

109 In spite of this, most studies recommend the use of altitude as the basic variable for
110 interpolation at regional and seasonal scales. This is the case for procedures
111 implemented in the Precipitation-elevation Regressions on Independent Slopes
112 Model (PRISM) to estimate fields of precipitation across conterminous North
113 America (Daly et al., 2017, 2008 and 1994).

114 Precipitation-elevation regressions were also used in Spain in combination with an
115 Inverse Distance Weighting (IDW) algorithm to create the monthly precipitation maps
116 that were used as input to the distributed hydrological model SIMPA with the
117 objective of analyzing water resources distribution in Spain (MAGRAMA, 2004). To
118 reflect orographic influence and the underestimation of precipitation given, a
119 collation of pseudo precipitation records was then added to original records. Pseudo
120 precipitation records were estimated by linear regression analyzed in certain

121 Spanish regions (Estrela et al., 1999, Álvarez-Rodríguez et al., 2017). Regions of
122 approximately 5,000 km² were delimited considering windward and leeward
123 location. A criterion to control the accuracy of interpolated precipitation was obtained
124 from the comparison of recorded runoff volume and the precipitation excess. But
125 uncertainties were revealed when considering the quality of flow data and the
126 calculus of base flow, abstractions and direct runoff. Moreover, the procedure
127 followed in MAGRAMA (2004) was considered inadequate and tedious to update the
128 water resources assessment and therefore, the updating of the pseudo precipitation
129 data.

130 Rainfall-runoff models have been used to estimate natural water resources
131 (unaltered) across the Spanish territory (Álvarez-Rodríguez et al., 2016; MAGRAMA,
132 2004). On the Iberian Peninsula, moist air masses from the Atlantic Ocean constitute
133 the most important source of precipitation, while the spatial distribution of
134 precipitation is a function of orography and direction of air flow. The influence of the
135 Mediterranean Sea in precipitation occurrence is also important as reflected in the
136 regional change of the seasonal precipitation pattern to maxima occurring in autumn
137 and spring.

138 Álvarez-Rodríguez et al. (2017) described some basis to improve spatial estimates
139 of rainfall for the Iberian Peninsula and Spanish Islands. They concluded that
140 precipitation over this territory depends on its complex orographic structure and
141 predominant weather types. Altitude and orientation are the main physiographic
142 factors that would help to estimate precipitation. In Spain, precipitation tends to be
143 positively correlated with altitude although this relationship varies depending on
144 seasonality and location. Annual precipitation lapse rates (PLR) were found to range

145 from 0.3 to 1.2 mm/m, reaching 1.5 mm/m in the Northern Iberian Peninsula and
146 diminish at higher altitudes (Álvarez-Rodríguez et al., 2017). This would justify the
147 use of non-linear functions in precipitation-altitude regression analysis as it will be
148 shown in this paper. In coastal areas, large precipitation increments or decrements
149 are found where small differences in altitude are given. Additionally, a source of
150 uncertainty is identified considering that precipitation is mostly recorded at low
151 elevations.

152 This paper proposes a hybrid model of interpolation at a regional scale that can be
153 used to derive high resolution fields of precipitation over territories with complex
154 orography. The interpolation model assumes two different components on monthly
155 precipitation. The first component reflects local and seasonal characteristics. It is
156 composed by 24 different monthly precipitation maps of means (12) and standard
157 deviations (12). It considers the varying influence of physiographic variables such as
158 altitude and orientation. The second precipitation component reflects the synoptic
159 pattern and it is composed by normalized anomalies derived from monthly
160 precipitation records and monthly means and standard deviations. The model
161 constitutes a comprehensive implementation considering the availability of historical
162 records and the need of avoiding slow calculations in large territories. This model
163 has been applied to estimate monthly precipitation maps of 200 m resolution for the
164 Iberian Peninsula, Balearic and Canary Islands, from October 1940 to September
165 2005. After the description of the database and data sources, the paper firstly
166 describes the procedure used for the estimation of the monthly precipitation patterns
167 and secondly, the interpolation of the anomalies of the precipitation records. The

168 analysis carried out to validate these procedures is also shown. To conclude, the
169 achievements of the hybrid interpolation model are remarked.

170 **2 Data Sources**

171 **2.1 Recorded ground series of rainfall**

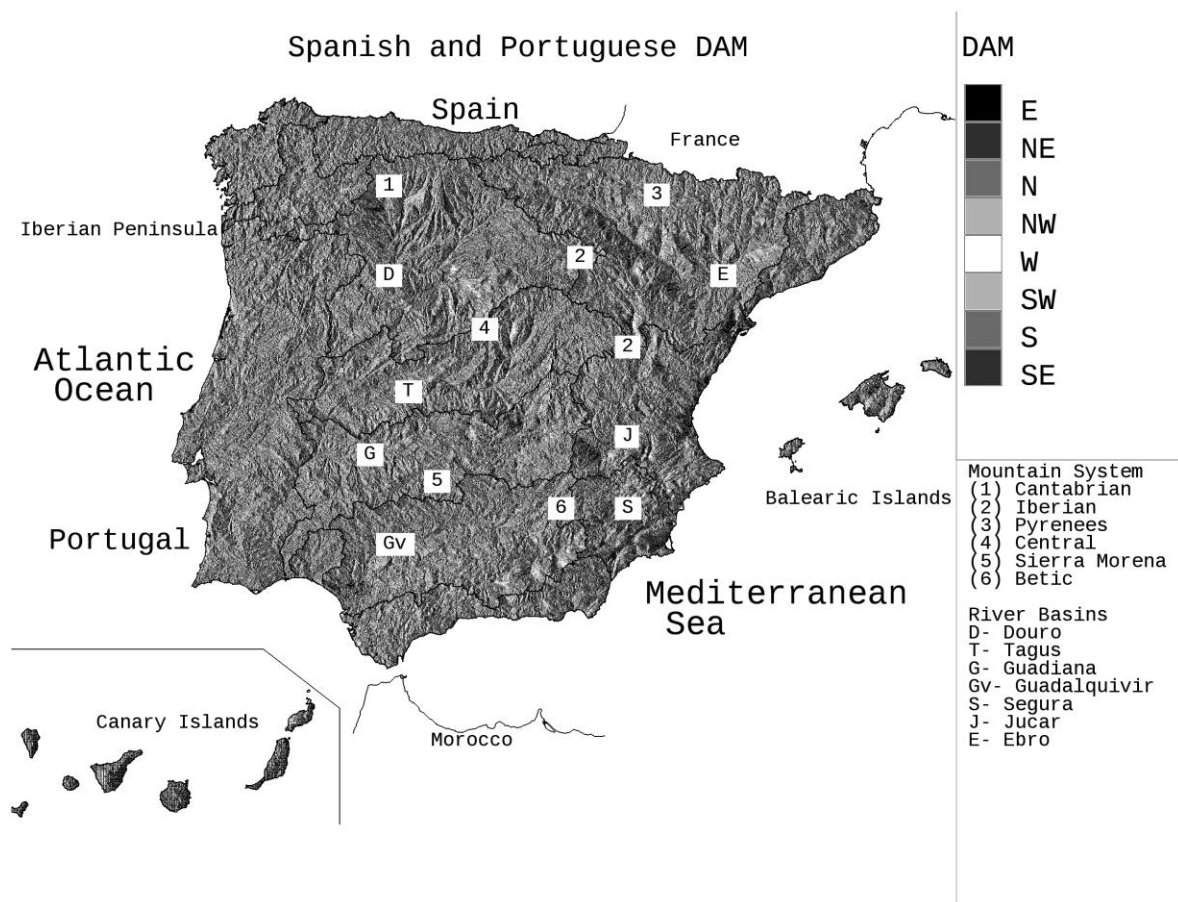
172 The databases of ground recorded precipitation were provided by the Spanish
173 Meteorological Office (AEMET) and the National Water Resources Information
174 System of the Portuguese Water Institute (SNIRH-INAG). Spanish data are supplied
175 by AEMET through its Virtual Office at <https://sede.aemet.gob.es/>. Portuguese data
176 are available at <https://snirh.apambiente.pt/>. The whole database of monthly
177 precipitation comprised 11,042 ground series from AEMET and 780 ground series
178 from SNIRH-INAG. Although some series comprise records from the 19th century
179 until the hydrological year 2004/05, the selected period is 1940/41-2004/05.

180 Existing gaps in recorded rainfall series were filled with regression-based data. Basis
181 of the completion model as well as a description of available data may be found in
182 Álvarez-Rodríguez et al. (2017).

183 **2.2 Location, elevation data and derived models**

184 Most of Spanish and Portuguese territories are a part of the Iberian Peninsula
185 (almost 582,000 km²), which is in southwestern Europe and surrounded by the
186 Atlantic Ocean and the Mediterranean Sea. This research encompasses the Iberian
187 Peninsula and the Balearic Islands in the Mediterranean Sea (5,000 km²) and the
188 Canary Islands (7,500 km²) in the Atlantic Ocean, which are influenced by a tropical
189 climate.

190 A Digital Elevation Model (DEM) has been composed joining Spanish and a
 191 Portuguese DEM to derive its main physiographic features as described in Álvarez
 192 Rodríguez et al. (2017). Figure 1 shows the Digital Aspect Model (DAM, cell angle
 193 at which terrain slope faces, counterclockwise from East) obtained considering
 194 relative elevation surrounding each cell of a DEM. This is done by means of the
 195 algorithm *r.slope.aspect* implemented in the GRASS-GIS (GRASS Development
 196 Team, 2012; Neteler and Mitsova, 2004).



197
 198 **Figure 1. Main Spanish mountain systems and hydrographic catchments are shown over a**
 199 **composition of Spanish and Portugal 200 m resolution DAM. Based on the UTM zone 30**
 200 **Geographical coordinates the Canary Islands are displaced 500,000 m East and 750,000 m**
 201 **North to encompass the whole geographical territory in a workable layout.**

202 **3 The Hybrid Model for Interpolation**

203 **3.1 Rationale**

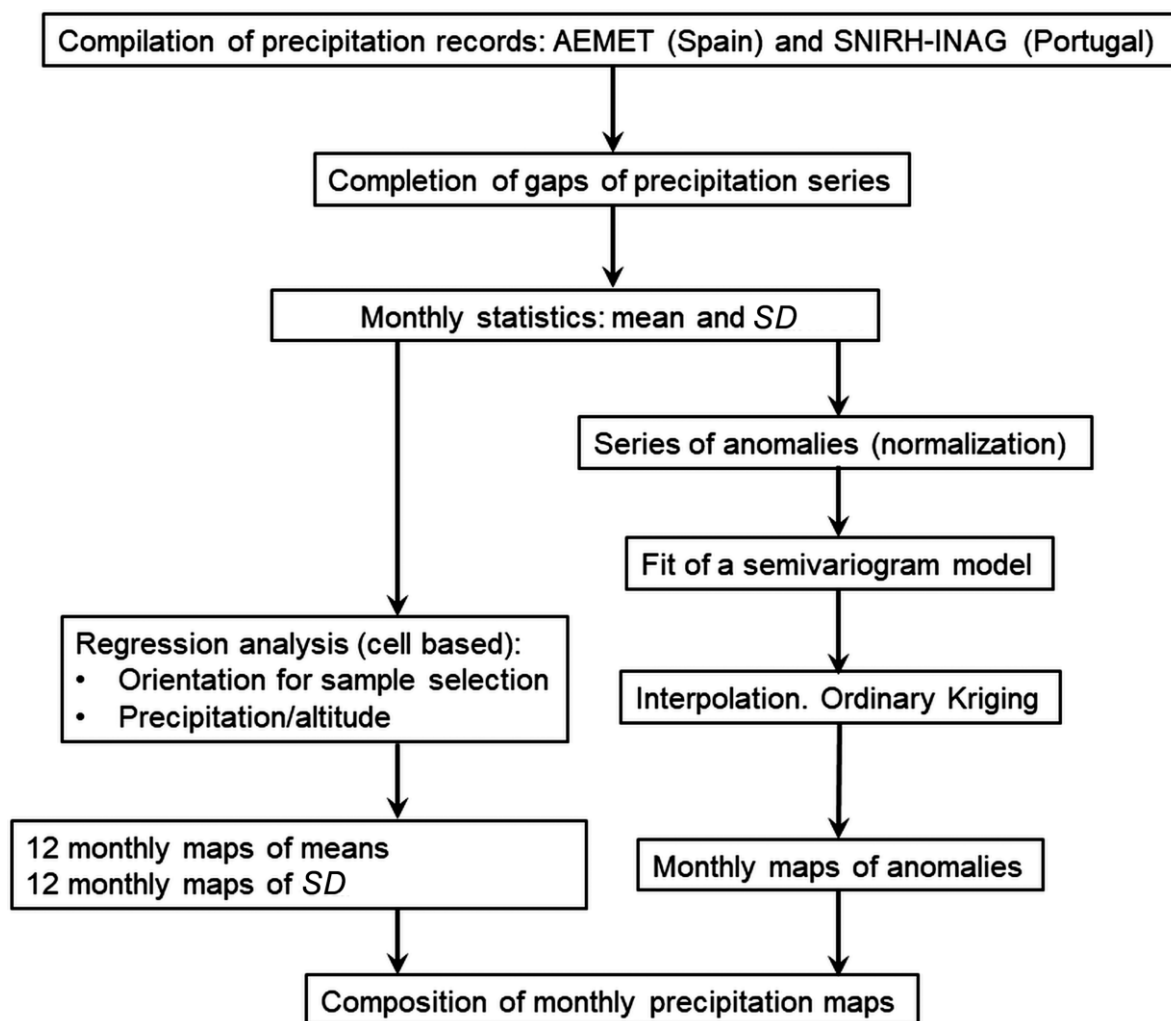
204 The following 5 points are some preliminary requirements adopted for the
205 development of an interpolation model to estimate monthly precipitation maps for the
206 territory with a 200 m resolution:

- 207 1. The number of records to be interpolated varies from month to month;
- 208 2. The selection of records to be interpolated should consider both the scarcity of
209 records in mountainous areas and the redundancies of records in lower altitudes;
- 210 3. Elevation and orientation are the predictive variables and their influences in
211 precipitation vary throughout the territory;
- 212 4. The interpolation model should be capable of working with different humid air
213 masses entering the territory and their different interactions with orography;
- 214 5. Finally, the time for calculation should be reduced enough considering the need
215 of deriving a whole set of 780 monthly interpolated maps of precipitation from
216 October 1940 to September 2005.

217 In accordance with these requirements, a hybrid interpolation model based on the
218 decomposition of temporal components used in synthetic series completion and
219 generation procedures has been proposed (Álvarez-Rodríguez et al., 2017; Salas et
220 al., 1980; Fiering and Jackson, 1971). It has been named “hybrid model” **because**
221 **two different interpolation models were implemented for two precipitation**
222 **components.**

223

224



225

226

Figure 2. Flow chart of methodology

227

Figure 2 shows a flowchart of the methodology applied. After the compilation of

228

records and completion of gaps in series of precipitation (Álvarez-Rodríguez et al.,

229

2017), monthly statistics of precipitation are estimated. The first component of

230

precipitation is composed by the monthly means and the monthly standard

231

deviations. Being the statistics that represent monthly centrality and variability, it is

232

considered that they represent the local influence on precipitation. The monthly step

233

accounts for seasonality.

234 The second component of monthly precipitation is represented by the anomalies
235 resulting from normalizing each monthly record of precipitation once monthly means
236 and standard deviations are known. The anomalies vary in time and would be
237 associated with the dominant synoptic circulation pattern each month. The following
238 sections describe in detail the algebra of each component. Regression analysis is
239 applied to derive monthly maps of means and standard deviations, while ordinary
240 kriging after an automated parameterization is applied on anomalies.

241 **3.2 Monthly Components of Centrality and Variability**

242 **3.2.1 Estimation of Local Patterns of Precipitation**

243 Local patterns of precipitation were represented by monthly mean and standard
244 deviation maps. Considering seasonal variability reflected in a monthly step, 24
245 different maps have been obtained by interpolation of monthly means (12 maps) and
246 monthly standard deviations (12 maps) derived from recorded series of precipitation
247 completed previously. Since orographic influence is variable, monthly means and
248 standard deviations were interpolated by means of regression analysis. Altitude was
249 used as a predictor in regression analysis. A regression equation was implemented
250 in each cell of the model. Samples were selected considering the orientation of the
251 place where each rain gauge station is located and distance from the center of a cell
252 to nearby rain gauge stations. Then, given the scarcity of records at higher altitudes,
253 a weighted regression equation was implemented to estimate precipitation to
254 prioritize nearby records close to a cell.

255 Statistics of recorded monthly rainfall series were calculated for the period ranging
256 between the hydrological years 1970/71 and 1999/00, which is the 30-year period of

257 maximum data availability (Álvarez-Rodríguez et al., 2017). The selection of a
258 unique period would assure homogeneity.

259 Monthly means and standard deviations were interpolated by a moving regression
260 equation based on altitude but using the orientation of the terrain as a criterion to
261 select the values of the sample to estimate each cell value.

262 The statistics obtained are georeferenced by means of the coordinates of each rain
263 gauge station. Then a selection of statistics is made for each cell based on distance
264 and orientation. Particularly, those rain gauge stations located over cells whose
265 orientation (DAM of 200 m resolution) is included in the 180° semicircular sector
266 formed by the orientation angle of the estimation cell and a semi-amplitude of $\pm 90^\circ$
267 are selected. It has been verified that semi-amplitude of less than 45° reduces
268 excessively the number of records to formulate each regression equation; and larger
269 semi-amplitudes, that is to say, between 45° and 90° , do not cause significant
270 differences to the 90° finally chosen. If a cell's slope is less than 1%, it is considered
271 that the orientation is not meaningful and rain gauge stations were selected
272 depending only on the distance. The maximum search distance from the center of
273 each cell is 100 km, or even larger till a minimum of 12 stations is found. The
274 maximum number of stations for each sample is 18.

275 Then, a cell precipitation-altitude regression equation is fitted according to a moving
276 weighted regression interpolation model (Lloyd, 2005; Naoum and Tsanis, 2004b;
277 Daly et al., 1994). Each cell-regression equation is fitted by the minimum least
278 squares criteria, independently of the equation fitted in nearby cells.

279 A simple linear regression equation between altitude and precipitation would involve
280 the extrapolation of PLR estimated at medium and low altitudes where precipitation

281 is mostly recorded. To improve estimations, logarithmic transformations have been
282 used to reduce or extend the scale of the transformed variable.

283 Four laws have been formulated to be applied considering the more suitable variable
284 to transform (precipitation or altitude) and the positive or negative correlation of
285 precipitation and altitude.

286 1. Logarithmic transformation of altitude (Eq. 1). It has the property of extending
287 the scale of the variable altitude in its lower levels and of reducing it in medium
288 to high elevations. Therefore, when the altitude-precipitation correlation is
289 positive, this transformation imposes a convex curvature, which is in
290 accordance with simplified theoretical approaches that describe a decrease
291 in PLRs with altitude due to depletion of available humidity. This
292 transformation is also applied in coastal areas where a negative correlation
293 and a high variability of precipitation with respect to altitude happens. The
294 relationship between altitude and precipitation is then given by Eq. (1):

$$295 \quad P(X, Y) = a \cdot \log[Z(X, Y)] + b \quad \text{Eq. (1)}$$

296 where $Z(X, Y)$ is the predictive variable in a cell of geographic coordinates X
297 and Y , $P(X, Y)$ is the recorded precipitation in that particular cell, a and b the
298 parameters of the simple regression equation fitted by minimum least
299 squares.

300 Then, the criterion to choose this case is that the altitude-precipitation
301 correlation is positive and the average altitude of the sample is lower than the
302 altitude of the cell. That is because it is considered that there are more records
303 at low levels to estimate rain at higher levels. Moreover, this transformation is
304 also applied when the correlation is negative and the average altitude of the

305 sample is higher than that of the cell to be estimated because it is considered
306 that there are more records at higher levels.

307 2. Logarithmic transformation of precipitation (Eq. 2). This transformation
308 weakens the decrease in precipitation when the altitude-precipitation
309 correlation is negative avoiding the extrapolation of negative PLRs from the
310 coast to the inner territories. This typically occurs in coastal areas. It is also
311 applied with positive PLRs where it is necessary to soften the reduction of
312 rainfall. The relationship between altitude and precipitation is then given by
313 Eq. 2:

$$314 \quad \log[P(X, Y)] = a \cdot Z(X, Y) + b \quad \text{Eq. (2)}$$

315 Then, the criterion to choose this case is that the altitude-precipitation
316 correlation is negative and the altitude of the cell is higher than the averaged
317 elevations of the sample. Likewise, this transformation is applied if positive
318 correlation and cell's altitude is lower than the averaged altitudes of the
319 sample. It should be emphasized that the effect of the logarithmic
320 transformation on precipitation is less significant, not only because the
321 sensitivity of the results is lower with reduced precipitation, but also because
322 in areas of low altitude, the density of the precipitation network is generally
323 higher.

324 Being z the predictive variable altitude ($Z(X, Y)$) or its transformed ($\log(Z(X, Y))$) in
325 a cell of coordinates X and Y , p the variable precipitation ($P(X, Y)$) or its transformed
326 ($\log(P(X, Y))$), i the indicative sub-index of each statistic of a sample of size N ($i =$
327 $1..N$) and w_i the weight given to each statistic, the parameters a and b of the
328 regression equation are obtained according to Eq. (3).

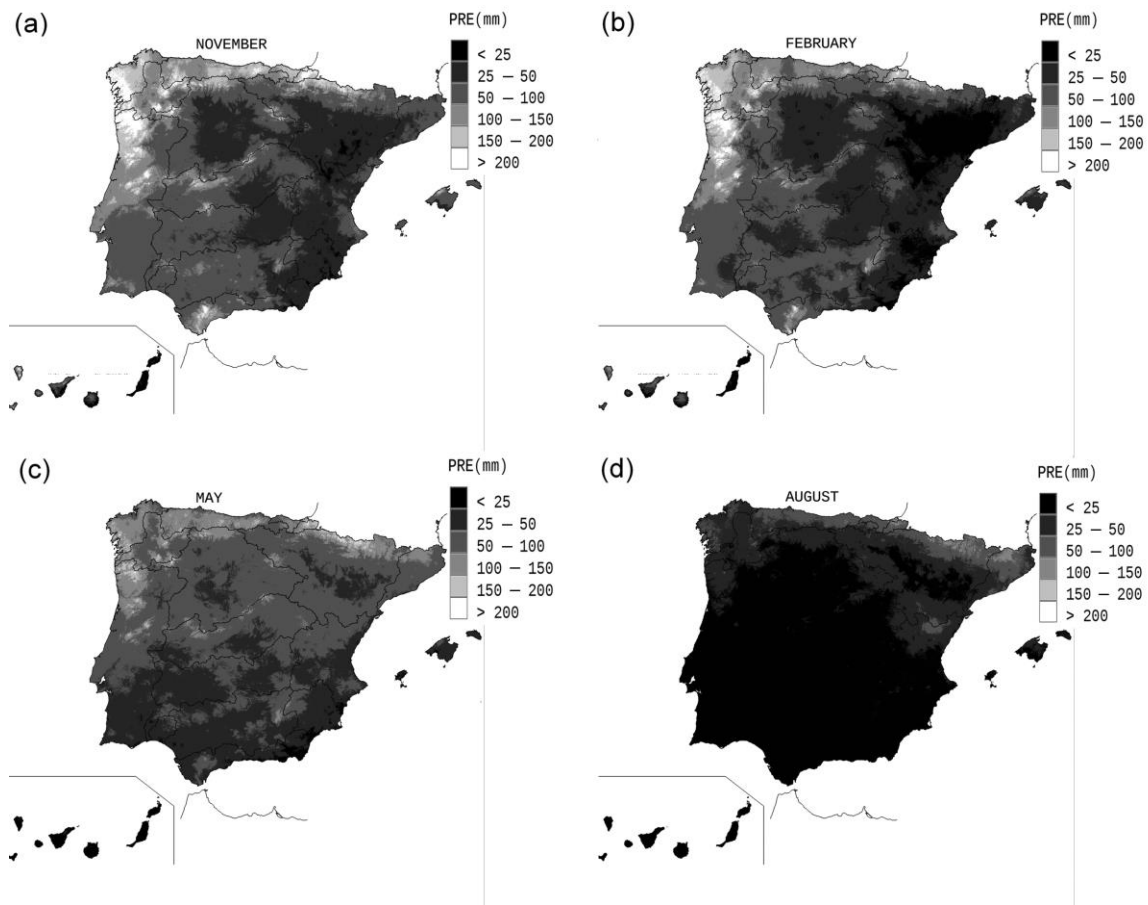
329
$$p = a \cdot z + b \quad a = \frac{\sum_{i=1}^N w_i \cdot z_i \cdot p_i - \sum_{i=1}^N w_i \cdot z_i \cdot \sum_{i=1}^N w_i \cdot p_i}{\sum_{i=1}^N w_i \cdot z_i^2 - (\sum_{i=1}^N w_i \cdot z_i)^2}$$

330
$$b = \sum_{i=1}^N w_i \cdot p_i - \frac{\sum_{i=1}^N w_i \cdot z_i \cdot p_i - \sum_{i=1}^N w_i \cdot z_i \cdot \sum_{i=1}^N w_i \cdot p_i}{\sum_{i=1}^N w_i \cdot z_i^2 - (\sum_{i=1}^N w_i \cdot z_i)^2} \quad \text{Eq. (3)}$$

331 The weight w_i assigned to station i is calculated with an inverse distance function of
 332 exponent h (Eq. 4). h takes the value of 2 after verifying that no significant differences
 333 are obtained between the results obtained with the frequent values, 1, 2 or 3. The
 334 distance d_j from i to j rain gauge station is calculated from the center of the coordinate
 335 cell (X, Y, Z) to each one of the N data selected (X_j, Y_j, Z_j) .

336
$$w_i(X, Y) = \frac{1}{\sum_j \frac{1}{d_j^h(X, Y, Z)}} \quad d_j = \sqrt{(X_j - X)^2 + (Y_j - Y)^2 + (Z_j - Z)^2} \quad \text{Eq. (4)}$$

337 Considering the interpolation in the Iberian Peninsula, Balearic and Canary Islands,
 338 a number of about 15,000,000 cells and, consequently, regression equations were
 339 fitted per month. Figure 3 shows 4 mean monthly precipitation maps representative
 340 of the 4 seasons of a year. They were obtained from the monthly means of 30 years
 341 of precipitation records between the hydrological years 1970/71 and 1999/00.

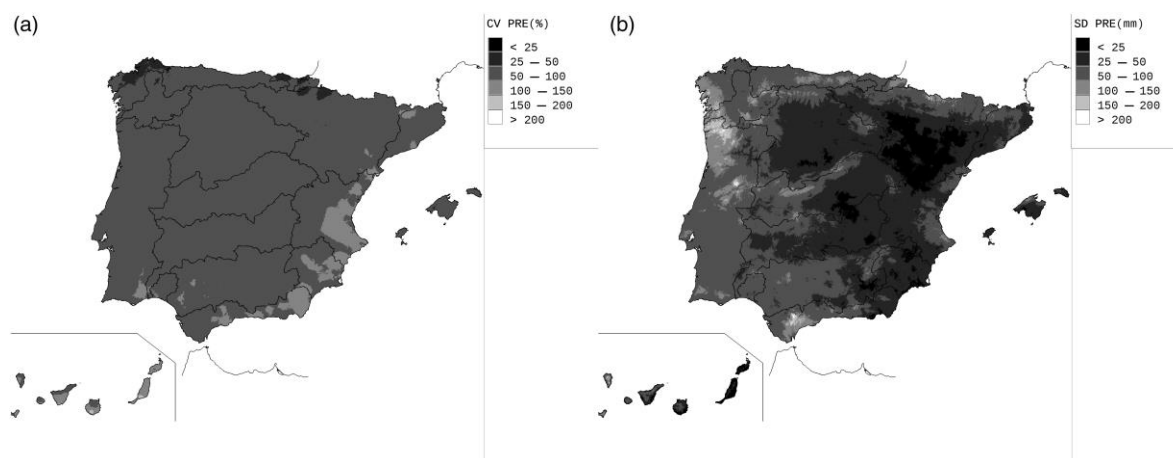


342

343 **Figure 3. Monthly mean precipitation maps of November (a), February (b), May (c) and**
 344 **August (d) considering the 30 years period from 1970/71 until 1999/00**

345 Monthly mean and standard deviation maps may be interpolated following the
 346 methodology shown previously. But once interpolated means are calculated, maps
 347 of standard deviations may benefit both from the high correlation coefficients
 348 achieved between the monthly means and monthly standard deviations and from the
 349 softened spatial variability across the territory shown by their ratio, the monthly
 350 coefficient of variation, CV (Álvarez-Rodríguez et al., 2017). The softened spatial
 351 variability is a useful property to interpolate the 12 monthly CVs if assuming a local
 352 stationarity and implementing an ordinary kriging model (OK) based on an
 353 omnidirectional semivariogram (Isaaks and Srivastava, 1989). Figure 4 shows the

354 monthly standard deviation maps obtained as a product of mean monthly
355 precipitation maps by the monthly coefficient of variation estimated by OK.



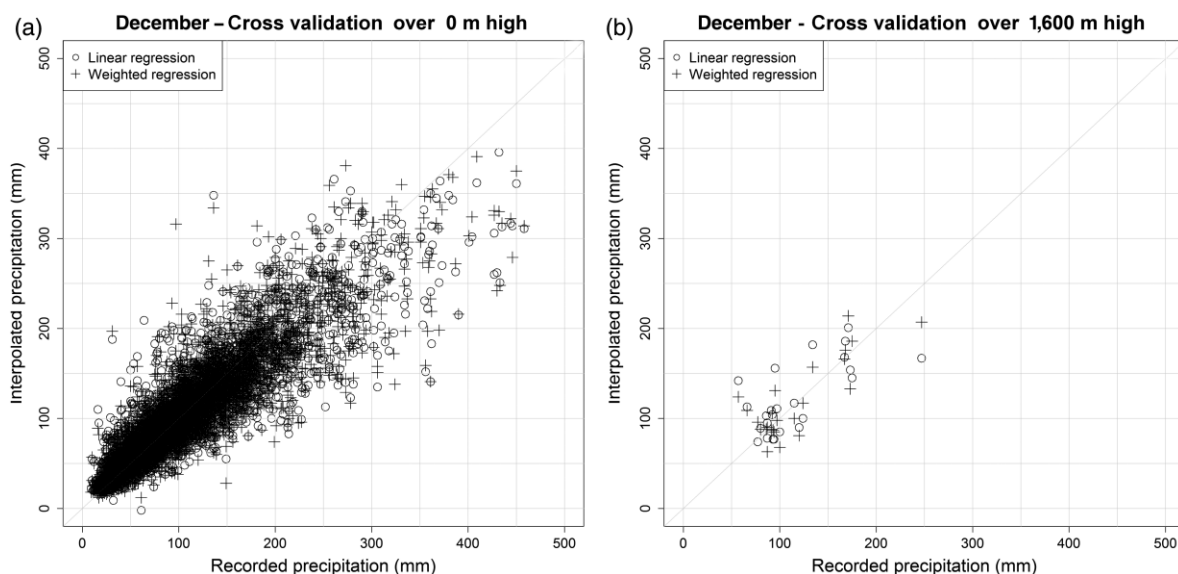
356

357 **Figure 4. Monthly Coefficient of Variation (CV) (a) and Standard Deviation (SD) (b) Maps of**
358 **November**

359 **3.2.2 Validation of Mean Monthly Maps**

360 A topic for discussion is the validation procedure followed to determine the goodness
361 of the precipitation maps obtained. A basic criterion is the comparison with previous
362 estimations. However, precedent estimations are also influenced by several sources
363 of errors. The present methodology improves the method based solely on distances
364 to nearest records that was applied in the MAGRAMA report (2004) as interpolation
365 procedure. MAGRAMA (2004) was the starting point of this present work, aimed to
366 develop a new model not only dependent on distances. Likewise, the Digital Climatic
367 Atlas of the Iberian Peninsula published by Ninyerola et al. (2007 and 2005) and the
368 Iberian Climatic Atlas published by AEMET (2011) were not available in a digital
369 format. However, the visual comparison with the AEMET (2011) most recent
370 estimation allowed concluding the agreement between the distributions of the
371 monthly means of precipitation obtained.

372 Cross validation is a technique used to estimate the error of interpolation. A
373 measurement of error is calculated from the comparison of each record against the
374 value resulting from the interpolation using the rest of the records (Falivene et al.,
375 2010; Isaaks and Srivastava, 1989). Figure 5 shows two scatterplots of mean
376 monthly precipitation recorded in December and that estimated by the moving
377 weighted regression interpolation procedure described in this paper, once the
378 logarithmic transformations and the weighting technique have been applied. The
379 scatterplots of the rest of the 11 months are similar, although quantities of
380 precipitation vary. The first scatterplot (left) represents the dispersion of the complete
381 sample of records in the Iberian Peninsula. The second one (right) shows the
382 dispersion of a sample corresponding to stations located at an altitude of more than
383 1,600 masl (Figure 5).



384

385

386 **Figure 5. Scatterplots of recorded and interpolated monthly precipitation (December)**

387 **considering a linear regression and a weighted linear regression on transformed**

388 **precipitation. The whole dataset in the Iberian Peninsula (a); records over a 1,600 m high (b)**

389 Figure 5 shows that both the linear regression method and the transformed-weighted
 390 method underestimate monthly precipitation at higher locations, particularly over 300
 391 mm of precipitation. However, this bias is lower at higher elevations when the
 392 transformed-weighted method is applied. Table 1 shows the mean relative errors
 393 (MRE) obtained for the Iberian Peninsula when the linear regression (LR) and the
 394 regression with logarithmic transformation and weighting (WR) are applied. The
 395 MRE is calculated based on the relative error (RE) of the series i , where $i = 1..N$
 396 where N is the total number of series (observatories) in the sample (Eq. 5).

397
$$RE_i = \frac{P_i^{interpolated} - P_i^{recorded}}{P_i^{recorded}} \% \quad MRE = \sum_{i=1}^N \frac{RE_i}{N} \quad \text{Eq. (5)}$$

398

	%	October	November	December	January	February	March	April	May	June	July	August	September
Over 0 m high	LR	4.38	5.90	6.03	5.73	6.79	5.91	3.98	3.69	6.96	7.77	11.99	6.44
	WR	2.70	3.66	3.40	3.19	3.96	3.54	2.24	2.21	4.91	2.86	7.90	4.74
Over 1,600 m high	LR	9.35	11.02	11.21	19.58	24.37	15.09	9.25	13.62	28.15	27.05	39.66	8.33
	WR	6.10	5.59	6.69	12.47	17.54	10.59	5.11	7.23	14.20	12.11	21.20	-0.10

399

400 **Table 1. Monthly MRE (%) obtained for the Iberian dataset considering Linear Regression**
 401 **(LR) estimation and the Logarithmic Transformation and Weighted Regression (WR)**

402 Based on the above, the logarithmic transformation and data weighting reduces the
 403 bias at high levels, in spite of the uncertainties due ultimately to the scarcity of
 404 information at the highest levels, whatever the chosen procedure is. The
 405 improvement obtained in areas of higher altitudes is considered to be related with
 406 the management of the PLR variability depending on altitude. The weighting
 407 technique applied gives more weight to nearest data and correct the higher PLR
 408 estimated at lower altitudes. So, this conclusion validates the use of the
 409 transformation and weighting techniques.

410 3.3 Monthly Anomalies of Recorded Rainfall

411 3.3.1 Definition and Estimation

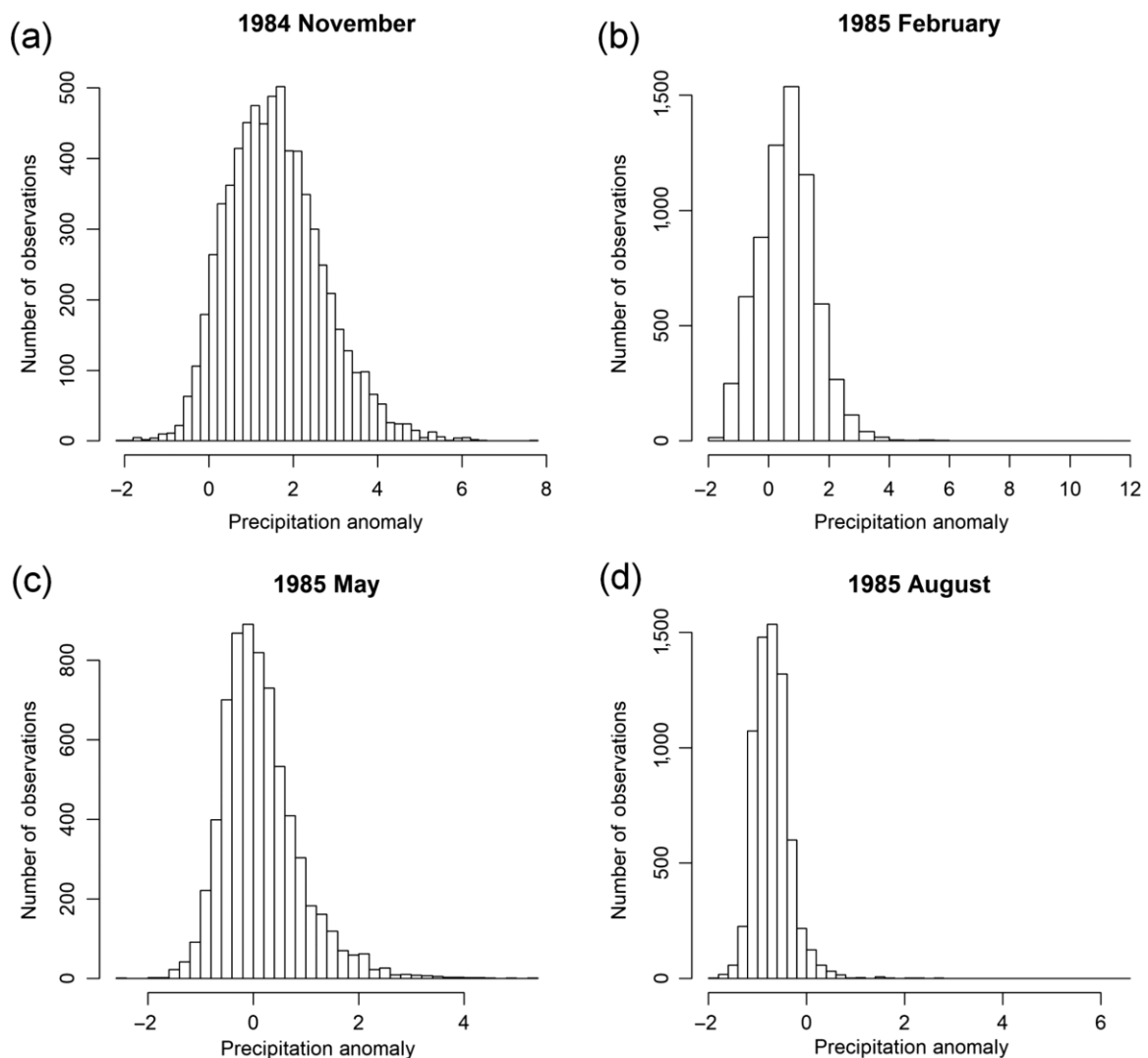
412 The moving weighted regression interpolation procedure could also be applied in a
413 monthly step from October 1940 to September 2005. Then, a total number of 780
414 monthly precipitation maps would have been obtained. But the computation time was
415 considered too long. The hybrid model proposed in this paper only uses the moving
416 weighted regression interpolation model to estimate 12 maps of monthly mean
417 patterns and another 12 of standard deviations. Then it is proposed to implement a
418 second model to interpolate the anomalies derived from each monthly precipitation
419 record and the calculated statistics. Considering the applicability to large sets of
420 maps, the reduction of the computational effort is a basic criterion when selecting an
421 interpolation procedure.

422 As previously defined, monthly anomalies would represent the variability given by
423 synoptic circulation patterns in a particular month of a year with respect to local
424 variability characterized by monthly means and standard deviations. Monthly
425 anomalies are calculated using the standardization formula (Eq. 6). Given a recorded
426 series of precipitation and being μ_i and σ_i the mean and standard deviation at month
427 i , the anomaly, $r_{i,j}$, of precipitation for the i month and j year, $P_{i,j}$, is given by Eq. 6.

$$428 \quad r_{i,j} = \frac{P_{i,j} - \mu_i}{\sigma_i} \quad \text{Eq. (6)}$$

429 Then monthly anomalies from October 1940 to September 2005 were calculated for
430 each rain gauge. Figure 6 shows the histogram of the complete set of anomalies of
431 the Iberian Peninsula in November 1984. They are supposed to reflect a synoptic
432 pattern being dominant in a particular month of a year. A similar histogram may be

433 obtained for each month of the period considered. Generally speaking, the
434 histograms show a central body of values with normal appearance and symmetry
435 around the central value, but there are also cases with a positive bias as a
436 consequence of the autumnal precipitation maxima in the Eastern areas of the
437 Peninsula (Figure 6). Some other histograms show negative extremes derived from
438 the transformation of precipitation values close to zero and low monthly deviations.
439 This is usually the case in the summer.



440

441

442 **Figure 6. Histograms of Precipitation Anomalies for November 1984 (a), February 1985 (b),**

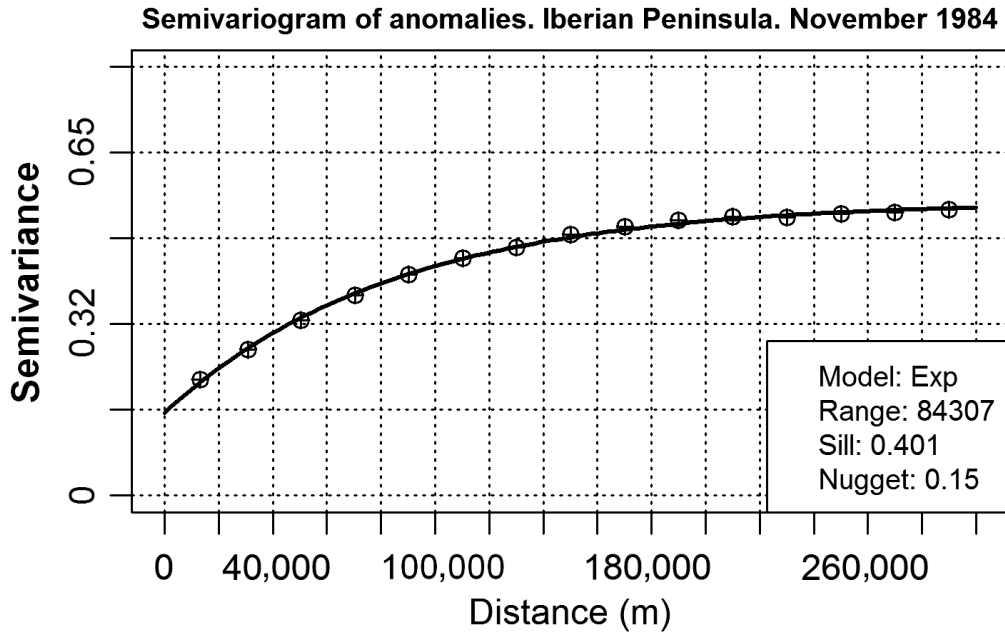
443 **May 1985 (c) and August 1985 (d)**

444 Kriging and the analysis of the spatial continuity of data is used to interpolate maps
445 of anomalies. They have a structural component of continuity that would be
446 represented by means of an omnidirectional semivariogram. If monthly sample of
447 anomalies show asymmetry and bias, then a Box-Cox transformation is applied to
448 facilitate the interpolation and to reduce the sensitivity to the extremes. The well-
449 known Box-Cox transformation (Eq. 7) depends on a parameter λ fitted to minimize
450 the coefficient of asymmetry of a sample.

451
$$\lambda \neq 0 \Rightarrow y = \frac{x^\lambda - 1}{\lambda} \quad \lambda = 0 \Rightarrow y = \ln(x) \quad \text{Eq. (7)}$$

452 **3.3.2 Interpolation of Anomalies**

453 The geostatistical analysis of monthly anomalies was carried out using the statistical
454 software R and the *gstat* package (Gräler et al., 2016, R Development Core Team,
455 2008, Pebesma, 2004). This software implements an automatically fitted
456 semivariogram model using ordinary least squares criteria. Then, a set of monthly
457 semivariograms is obtained for the period 1940/41-2004/05 in each of the 3 regions
458 considered, Iberian Peninsula, Balearic and Canary Islands. The chosen
459 semivariogram function is the exponential one. Parameters representing the spatial
460 continuity are the nugget effect, the sill and the range (Figure 7).



461

462 **Figure 7. Semivariogram of Iberian Peninsula anomalies of November 1984 fitted to an**
 463 **exponential one**

464 Most semivariograms behave in the same way as the one shown in Figure 7.
 465 Nevertheless, some others show greater variability and oscillations. Table 2 shows
 466 the median of each of the 3 parameters (nugget, sill and range) of the exponential
 467 semivariograms fitted from October 1970 to September 2000. Sill and range values
 468 seem to fit higher values during the rainy season that, in the Mediterranean area
 469 correspond to spring and autumn, while in the Atlantic it extends from autumn to
 470 spring.

	October	November	December	January	February	March	April	May	June	July	August	September
Iberian Peninsula												
	0.05	0.05	0.05	0.05	0.06	0.06	0.06	0.06	0.07	0.05	0.05	0.05
	0.12	0.14	0.09	0.08	0.13	0.10	0.13	0.13	0.08	0.07	0.07	0.08
	82	101	89	74	96	76	96	58	54	45	54	50
Balearic Islands												
	0.04	0.04	0.10	0.02	0.05	0.07	0.06	0.08	0.05	0.05	0.07	0.02
	0.37	0.28	0.49	0.22	0.19	0.42	0.27	0.41	0.36	0.38	0.40	0.32
	19	30	84	32	55	38	104	179	45	18	30	57
Canary Islands												
	0.06	0.01	0.07	0.00	0.00	0.02	0.12	0.15	0.14	0.04	0.10	0.07
	0.20	0.15	0.19	0.12	0.21	0.20	0.27	0.16	0.16	0.05	0.07	0.21
	15	15	19	9	11	11	60	25	60	60	63	18

472

473 **Table 2. Median of semivariogram parameter values found for the collation of anomalies**
474 **obtained from October 1970 to September 2000**

475 Ordinary kriging (OK) was used to interpolate anomalies taking into account that this
476 model may operate with local stationarity. It also weights data to diminish the
477 influence of redundancies (Isaaks and Srivastava, 1989). Finally, OK shows a
478 conceptual equivalence with other deterministic models such as the variational
479 approach by means of regularized spline with tension (RST) (Mitas and Mitasova,
480 1988). The next section evaluates the OK benefits in respect of the simpler but much
481 faster IDW as well as the similarities given by a RST approach.

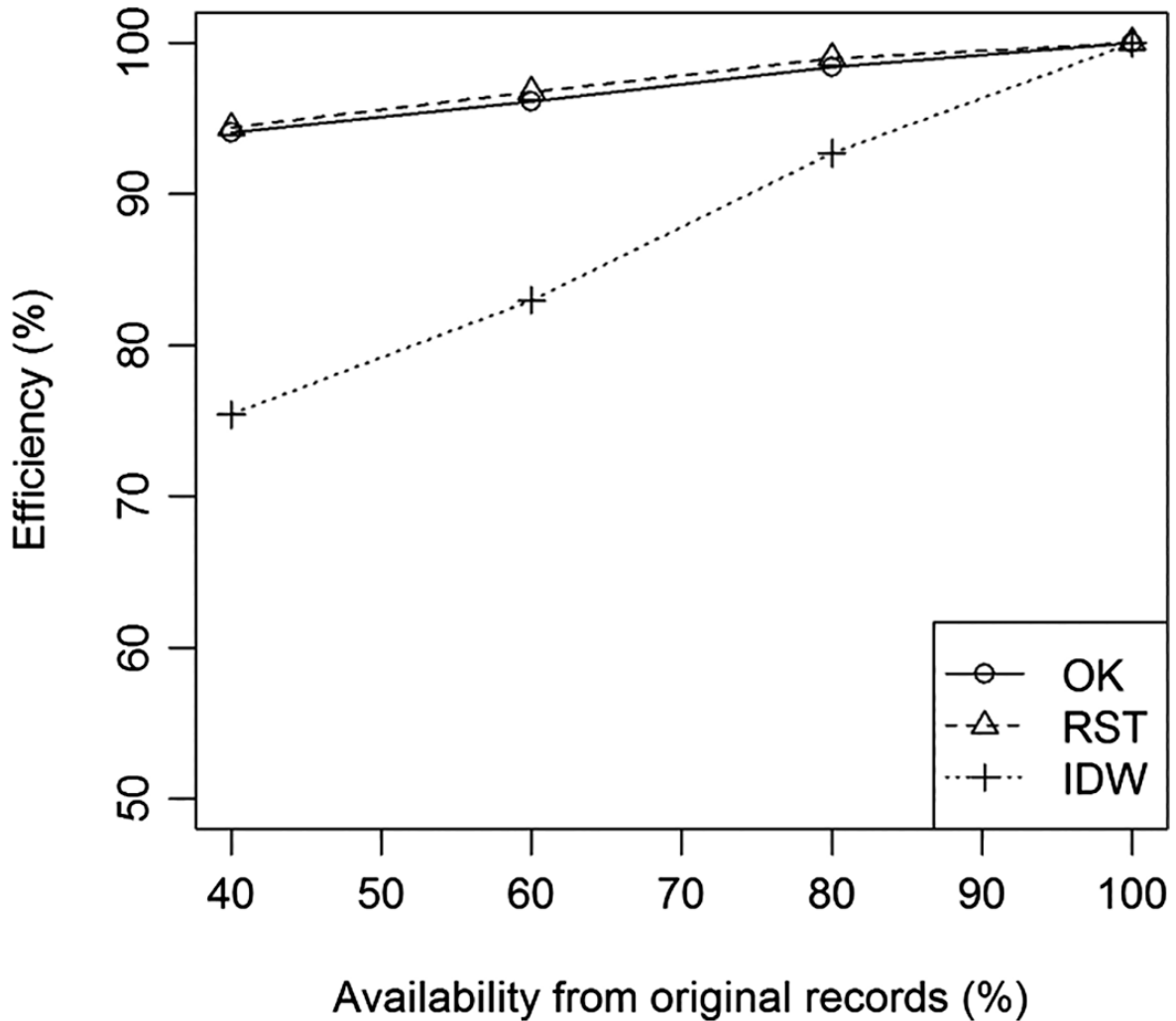
482 **3.3.3 Interpolation Efficiency**

483 The goodness of the interpolation methods applied on anomalies has been
484 evaluated through the loss of efficiency obtained when the available data is reduced.
485 Thus, a percentage of rain gauge stations (i.e., their series of anomalies) was
486 randomly selected and removed from the original sample. Then, the available set of
487 monthly maps is interpolated and an efficiency coefficient map is obtained. The
488 efficiency coefficient is then associated to the interpolation model used. Eq. 8
489 describes the formula used to obtain the efficiency coefficient in each cell.

$$490 \quad CE = \frac{\sum_{i=1}^n (r_i - m_r)^2 - \sum_{i=1}^n (s_i - r_i)^2}{\sum_{i=1}^n (r_i - m_r)^2} \quad \text{Eq. (8)}$$

491 where s_i are the mean monthly maps of anomalies for each i year (from 1 to n)
492 derived from the use of an interpolation model. Taking into account that 3 different
493 interpolation models are used (IDW, RST and OK), 3 different sets of maps are
494 estimated. The percentages of reduction from the complete set of rain gauge stations

495 are 60%, 40% and 20%. That is to say that the 3 interpolation models are applied to
 496 3 different sets that are equivalent to the use of 40%, 60% and 80% in respect of the
 497 complete set of series. r_i is the mean monthly map of anomalies for each year i
 498 interpolated by means of IDW, RST and OK, but for the whole set of series (i.e., a
 499 100% of availability); m_r is the mean map of r_i .



500

501

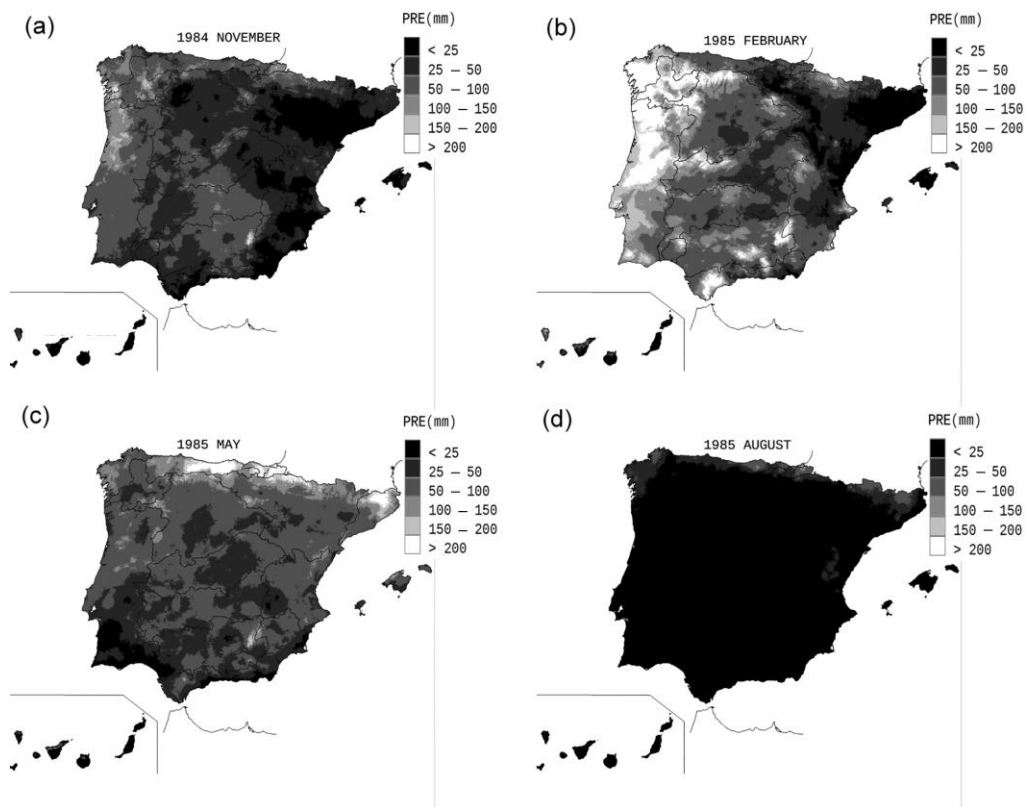
502 **Figure 8. Efficiency considering the interpolation method and a reduction in available**
 503 **records**

504 Figure 8 shows the averaged efficiency coefficient dependent on the interpolation
 505 model (OK, RST and IDW) and on the availability from the complete sample of

506 series. The faster loss of efficiency of the IDW is highlighted in respect of OK and
507 RST models. Thus, improvements in efficiency are linked to modeling the spatial
508 continuity as done in OK and RST models.

509 3.4 Hybrid Interpolated Monthly Precipitation Maps

510 Figure 9 shows a sequence of monthly rainfall maps interpolated during the
511 hydrological year 1984/85. These maps have been obtained by combining the
512 monthly maps of means and standard deviations, which would represent the local
513 anomalies, and the precipitation anomalies related to synoptic atmospheric
514 circulation. The "hybrid" model is finally composed by the use of the model of moving
515 weighted regression on transformed precipitation (presented in 3.2.1) and by the OK
516 to interpolate the precipitation anomalies (presented in 3.3.2).



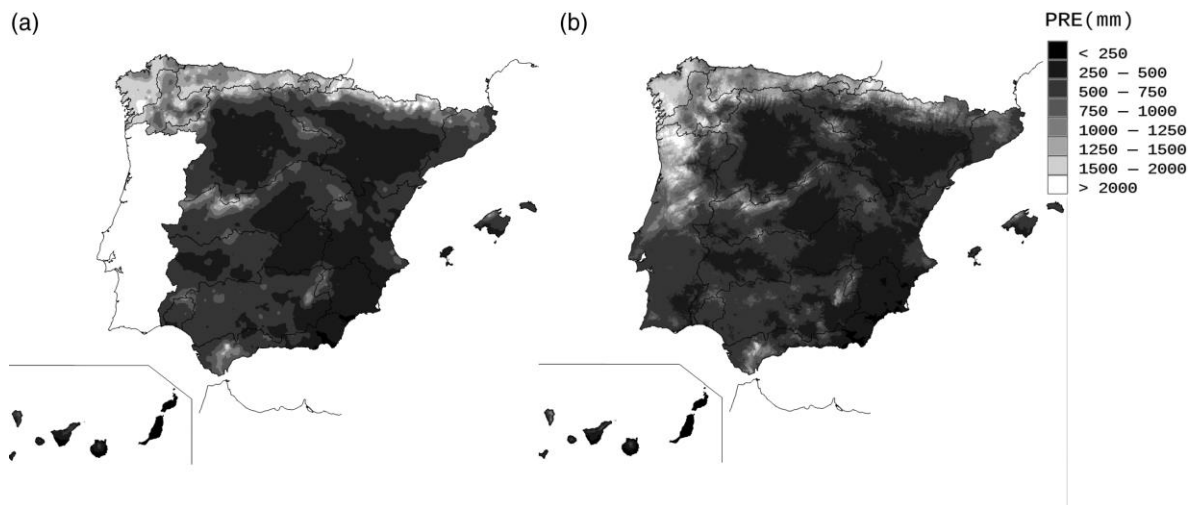
517

518 **Figure 9. Monthly precipitation maps interpolated by means of the hybrid model combining a**
519 **Moving Weighted Regression on transformed Precipitation for mean and standard deviation**

520 and Ordinary Kriging for anomalies. Maps from the hydrological year 1984/85: November
521 1984 (a), February 1985 (b), May 1985 (c) and August 1985 (d)

522 4 Results and discussion

523 A mean annual precipitation map is derived from the monthly set of estimates (Figure
524 10). Thus, the average annual precipitation is 655 mm/year. Although this figure is
525 only 4% less than the estimated precipitation map of MAGRAMA (2004), regional
526 and local differences are highlighted when the spatial distribution is considered.



527

528

529 **Figure 10. Mean annual precipitation maps (1940/41-1995/96) obtained by MAGRAMA (2004)**

530

(a) and by the implementation of the hybrid method (b)

531 The spatial distribution of precipitation maps in MAGRAMA (2004) is then attenuated
532 when compared to results obtained by the hybrid model where the orographic
533 structure is clearly remarked (Figure 10). Additionally, the isolation of certain data is
534 reflected in the IDW methodology followed by MAGRAMA (2004) by means of
535 rounded artifacts of interpolated precipitation while the help of orographic influence
536 and the modeling of the spatial continuity clearly improve the results obtained with
537 the hybrid model (Álvarez-Rodríguez, 2011). Furthermore, the spatial comparison of
538 the precipitation map obtained in MAGRAMA (2004) and the one presented in this

539 paper highlights several regional/local differences in precipitation amounts. Mostly,
540 in areas (see Figure 1) such as the upper Ebro River Basin and its left margin
541 (Pyrenees) as well as in the Cantabrian region of the Iberian Peninsula (Álvarez-
542 Rodríguez, 2011). Finally, the hybrid model has the advantage of managing
543 precipitation records in a systematic way avoiding the time and expertise needed in
544 MAGRAMA (2004).

545 A topic for discussion is constituted by the effect of resampling in estimated
546 precipitation. Greater resolution was resampled to 200 m to derive DEM in most of
547 the territory. The altitude of the rain gauge was used for the regression analysis, but
548 each cell altitude was used to estimate the precipitation of every cell. But a lot of
549 variability exists in mountainous areas that would influence the representation of cell
550 altitude and subsequently on estimated precipitation in every cell.

551 The set of monthly maps was implemented in a distributed hydrological model to
552 estimate water resources in natural regime in Spain. This fact implied the need to
553 reparametrize the hydrological model, opening the possibility of including
554 physiographic factors such as soil textures or slopes in the calibration of the
555 maximum soil storage capacity (Álvarez-Rodríguez et al., 2016). The need for a
556 parameterization emphasizes the importance of the spatial distribution of
557 precipitation and how the uncertainty is transferred to parameters of a hydrological
558 model.

559 **5 Conclusions**

560 A hybrid model to improve the estimation of monthly precipitation distribution in great
561 areas of complex orography has been proposed. It combines two interpolation

562 models applied to each one of the two main different components distinguished in
563 the precipitation.

564 Firstly, monthly means and standard deviations were interpolated by a moving
565 regression equation based on altitude but using the orientation of the terrain as a
566 criterion to select the values of the sample to estimate each cell value. The
567 regression also incorporates the use of transformation functions (logarithms of
568 precipitation or altitude) and weights as a function of the distance to prioritize nearby
569 information avoiding the overestimation at higher altitudes using records of lower
570 altitudes. Monthly maps of standard deviations can be either obtained by inferring
571 regression equations based on altitude and orientation or by the product of maps of
572 monthly variation coefficients by the already estimated maps of monthly means. Due
573 to the high correlation between means and standard deviations, its ratio (coefficient
574 of variation) does not show the spatial variability shown by the monthly means and
575 can be assumed locally stationary, which facilitates its estimation in large territories
576 through interpolation procedures such as ordinary kriging (OK). This first component
577 provides information about the seasonal variability of precipitation at local scale.

578 The second component of precipitation is constituted by the anomalies, that are
579 mainly related with synoptic situations that affect at regional scale. Its bias is
580 corrected to reduce the asymmetry of each sample and then interpolated in a
581 monthly step using an OK. A comparison between averaged efficiency coefficients
582 derived from OK, variational approach (RST) and inverse distance algorithm (IDW)
583 revealed how the implementation of a continuity structure in an interpolation model
584 benefits the results. It means that methods working with a spatial continuity structure
585 (OK and RST) are adequate to represent the precipitation in a complex terrain,

586 obtaining accurate estimations even when the loss of observatories reached a 60%.
587 Then, structures embedded in usual interpolation methodologies as OK and RST
588 may replace a high percentage of redundancies existing in a meteorological network.
589 In spite of this it is therefore necessary to insist on the need to improve the availability
590 of precipitation records at higher altitudes in order to reduce the uncertainty of
591 precipitation estimation.

592 The hybrid model presented in this paper has the advantage of **reducing the**
593 **computational time. An advantage of the linear regression method is its conceptual**
594 **simplicity, while accounting for the non-linear relationship between precipitation and**
595 **altitude.** However, when it must be repeatedly applied to large territories for a great
596 number of precipitation maps needed to subsequently force a hydrological model,
597 the long time for calculation **make its use makes the method unsuitable.** Therefore,
598 the hybrid approach limited its use to the estimation of the 24 maps of the monthly
599 means and standard deviations. Next, anomalies associated to regional components
600 are interpolated by means of OK after parameterizing the monthly semivariograms.
601 As seen, OK and RST account for spatial continuity, which is variable from month to
602 month and can be applied to a variable number of records without a significant loss
603 of information about precipitation performance.

604 The main advantage of the proposed methodology relies on that it has been
605 composed considering advantages of different procedures in order to represent
606 precipitation **both over large territories and complex terrain.** Regression analysis
607 considers precipitation/altitude relationships following usual procedures reviewed to
608 implement the non-linearity in a straightforward way. Anomaly interpolation takes the

609 advantage of automatic parameterization and methodologies capable of
610 implementing the spatial continuity.

611 **6 Acknowledgements**

612 The Spanish Meteorological Agency (AEMET), the Portuguese Water Institute and
613 the people maintaining HIDRO database of the Center of Hydrographic Studies of
614 CEDEX as well as the Spanish Water Directorate for promoting the Water Resources
615 studies in Spain for which this work was developed. This work has been partially
616 supported by the Spanish Project HOPE (CGL2014-52571-R) of the Ministry of
617 Economy, Industry and Competitiveness. The authors would also like to thank Maria
618 Sernequet Belda, from the Mediterranean Network of Basin Organizations, for her
619 constructive review of the English writing.

620 **7 References**

- 621 AEMET. 2011. Atlas Climático Ibérico. (Iberian Climate Atlas) VV.AA. Agencia
622 Estatal de Meteorología. Ministerio de Medio Ambiente. ISBN: 978-84-7837-
623 079-5. URL:
624 [http://www.aemet.es/documentos/es/conocermas/publicaciones/Atlas-](http://www.aemet.es/documentos/es/conocermas/publicaciones/Atlas-climatologico/Atlas.pdf)
625 [climatologico/Atlas.pdf](http://www.aemet.es/documentos/es/conocermas/publicaciones/Atlas-climatologico/Atlas.pdf)
626 Last Access: 14/02/2018
- 627 Álvarez-Rodríguez J, Llasat MC and Estrela T. 2017. Analysis of geographic and
628 orographic influence in Spanish monthly precipitation. Int. J. Climatol.
629 doi:10.1002/joc.5007
- 630 Álvarez-Rodríguez J, Barranco Sanz LM, García Bravo N, Potenciano de las Heras
631 Á, Villaverde Valero JJ. 2016. La Evaluación de Recursos Hídricos en España

632 (Water Resources Assessment in Spain). (In Spanish), July/2016, 380 p.
633 Centre for Hydrographic Studies of CEDEX ISBN/EAN: 9788477905783
634 Álvarez-Rodríguez J. 2011. Estimación de la distribución espacial de la precipitación
635 en zonas montañosas mediante métodos geoestadísticos (Analysis of spatial
636 distribution of precipitation in mountainous areas by means of geostatistical
637 analysis). PhD thesis. Polytechnic University of Madrid, Higher Technical
638 School of Civil Engineering
639 Barros AP, Kim G, Williams E and Nesbitt SW. 2004. Probing Orographic Controls
640 in the Himalayas During the Monsoon Using Satellite Imagery. Nat. Hazards
641 Earth Syst. Sci., 4, 29-51
642 Barstad I, Grabowski W and Smolarkiewicz P. 2007. Characteristics of large-scale
643 orographic precipitation: evaluation of linear model in idealized problems. J.
644 Hydrol., 340, 78-90
645 Bookhagen B and Burbank DW. 2006. Topography, relief and TRMM-derived rainfall
646 variations along the Himalaya, Geophys. Res. Lett., 33
647 Creutin JD and Obled C. 1982. Objective Analyses and Mapping Techniques for
648 Rainfall Fields: An Objective Comparison. Water Resour. Res., 18(2), 413-
649 431
650 Dhar ON and Nandargi S. 2004. Rainfall distribution over the Arunachal Pradesh
651 Himalayas. Weather, 59, 155-157
652 Daly C, Slater ME, Roberti JA, Laseter SH and Swift LW. 2017. High-resolution
653 precipitation mapping in a mountainous watershed: ground truth for
654 evaluating uncertainty in a national precipitation dataset. Int. J. Climatol.
655 doi:10.1002/joc.4986

656 Daly C, Halbleib M, Smith JI, Gibson WP, Doggett MK, Taylor GH, Curtis J and
657 Pasteris PP. 2008. Physiographically sensitive mapping of climatological
658 temperature and precipitation across the conterminous United States. *Int. J.*
659 *Climatol.*, 28, 2031-2064

660 Daly C, Neilson RP and Phillips DL. 1994. A Statistical Topographic Model for
661 Mapping Climatological Precipitation over Mountainous Terrain. *J. Appl.*
662 *Meteor.*, 33, 140-158

663 Estrela T., Cabezas F. and Estrada, F. 1999. La evaluación de los recursos hídricos
664 en el Libro Blanco del Agua en España (Water Resources Assessment in the
665 Water in Spain Book). *Revista de Ingeniería del Agua*, 6(2), 125–138, 1999

666 Falivene O, Cabrera L, Tolosana-Delgado R and Sáez A. 2010. Interpolation
667 algorithm ranking using cross-validation and the role of smoothing effect. A
668 coal zone example. *Computers and Geosciences*, 36 (4), 512-519

669 Fiering MB and Jackson BB. 1971. *Synthetic Stream Flows*, American Geophysical
670 Union, Washington D.C., 98 p.

671 Gambolati G and Volpi G. 1979. A conceptual Deterministic Analysis of the Kriging
672 Technique in Hydrology. *Water Resour. Res.*, 15(3), 625–629

673 Gómez-Hernández J, Cassiraga E, Guardiola-Albert C, Álvarez-Rodríguez J. 2001.
674 Incorporating Information from a Digital Elevation Model for Improving the
675 Areal Estimation of Rainfall. In *GeoENV III: Geostatistics for Environmental*
676 *Applications*. Monestiez, P., Allard, D., and Froidevaux, R., (ed.). Kluwer
677 Academic Publishers, Dordrecht, 67-78

678 Goovaerts P. 2000. Geostatistical Approaches for Incorporating Elevation into the
679 Spatial Interpolation of Rainfall. *J. Hydrol.*, 228 (1-2), 113-129

680 Gräler B, Pebesma E and Heuvelink G. 2016. Spatio-Temporal Interpolation using
681 gstat. *The R Journal* 8(1), 204-218

682 GRASS Development Team. 2012. Geographic Resources Analysis Support
683 System (GRASS) Software. Open Source Geospatial Foundation Project.
684 <http://grass.osgeo.org>

685 Hanson CL. 1982. Distribution and Stochastic Generation of Annual and Monthly
686 Precipitation on a Mountainous Watershed in Southwest Idaho. *JAWRA*
687 *Journal of the American Water Resources Association*, 18, 875-883

688 Hay LE, Viger R and McCabe G. 1998. Precipitation Interpolation in Mountainous
689 Regions Using Multiple Linear Regression: Hydrology, Water resources, and
690 Ecology in Headwaters, *Proceedings of the HeadWater'98 Conference*,
691 Kovar K, Tappeiner U, Peters NE and Craig RG. IAHS Publication (248), 33-
692 38

693 Isaaks EH and Srivastava RM. 1989. *An Introduction to Applied Statistics*. Oxford
694 University Press

695 Linsley RK, Kohler MA and Paulhus JLH. 1949. *Applied Hydrology*. McGraw Hill

696 Lloyd CD. 2005. Assessing the effect of integrating elevation data into the estimation
697 of monthly precipitation in Great Britain. *J. Hydrol.*, 308, 128-150

698 MAGRAMA. 2004. *Water in Spain*. Ministry of Agriculture, Food and Environment.
699 Technical Secretariat-General. Madrid. Spain

700 Marquínez J, Lastra J, García P. 2003. Estimation Models for Precipitation in
701 Mountainous Regions: the Use of GIS and Multivariate Analysis. *J. Hydrol.*
702 270, 1-11

703 Martínez-Cob A. 1996. Multivariate Geostatistical analysis of Evapotranspiration and
704 Precipitation in Mountainous Terrain. *J. Hydrol.*, 174 (1-2), 19-35

705 Mitas L and Mitasova H. 1988. General variational approach to the approximation
706 problem, *Computers and Mathematics with Applications*, 16, 983-992

707 Naoum S and Tsanis, IK. 2004a. Ranking Spatial Interpolation Techniques using a
708 GIS-based DSS. *Global Nest: the Int. J.* 6 (1), 2004, 1-20

709 Naoum S and Tsanis IK. 2004b. Orographic precipitation modeling with multiple
710 linear regression. *J. Hydrol. Eng.*, 9 (2), 79-102

711 Neteler M, Mitasova H. 2004. *Open Source GIS: A GRASS GIS Approach*. 2nd
712 edition. Kluwer Academic Publishers/Springer, Boston. 424 p.

713 Ninyerola M, Pons X and Roure JM. 2005. *Atlas Climático Digital de la Península*
714 *Ibérica. Metodología y aplicaciones en bioclimatología y geobotánica.*
715 *Universidad Autónoma de Barcelona, Bellaterra*

716 Ninyerola M, Pons X and Roure JM. 2007. Monthly precipitation mapping of the
717 Iberian Peninsula using spatial interpolation tools implemented in a
718 Geographic Information System. *Theor. Appl. Climatol.*, 89, 195-209

719 Pebesma EJ. 2004. Multivariable geostatistics in S: the gstat package. *Computers*
720 *& Geosciences*, 30, 683-691

721 R Development Core Team. 2008. *R: A language and environment for statistical*
722 *computing.* R Foundation for Statistical Computing, Vienna, Austria. ISBN 3-
723 900051-07-0, URL <http://www.R-project.org>

724 Rotunno R and Ferretti. R. 2001. Mechanisms of intense Alpine rainfall. *J. Atmos.*
725 *Sci.*, 58, 1732-1749

726 Salas JD, Delleur JW, Yevjevich V, Lane WL. 1980. Applied Modeling of Hydrologic
727 Time Series. Water Resources Publications. Fort Collins Colorado, U.S.A.,
728 484 p.

729 Singh P, Ramasastri KS and Naresh K. 1995. Topographical Influence on
730 Precipitation Distribution in Different Ranges of Western Himalayas. Nordic
731 Hydrology, 26 (4/5), 259-284

732 Tabios III GQ and Salas JD. 1985. A Comparative Analysis of Techniques for Spatial
733 Interpolation of Precipitation. JAWRA Journal of the American Water
734 Resources Association, 21, 365-380

735 Thiessen AH. 1911. Precipitation averages for large areas. Mon. Wea. Rev., 39,
736 1082-1089

737 Tobin C, Nicotina L, Parlange MB, Berne A and Rinaldo A. 2011. Improved
738 interpolation of meteorological forcings for hydrologic applications in a Swiss
739 Alpine region. J. Hydrol., 401 (1-2), 77-89

740 Weber DD and Englund EJ. 1992. Evaluation and comparison of spatial
741 interpolators. Mathematical Geology 24, 381-391

742 Weber DD and Englund EJ. 1994. Evaluation and comparison of spatial interpolators
743 II. Mathematical Geology 26, 589-603

744 World Climate Programme. 1985. World Meteorological Organization. Review of
745 Requirements for Area-Averaged Precipitation Data, Surface-Based and
746 Space-Based Estimation Techniques, Space and Time Sampling, Accuracy
747 and Error; Data Exchange. Boulder Colorado, EE.UU., 17-19

748 WMO. 1994. Guide to hydrological practices. WMO-168. Data acquisition and
749 processing, analysis, forecasting and other applications. 5th edition, 1994.
750 World Meteorological Organization. Geneva. ISBN: 92-63-30168-9